

# Separation of nematic and smectic-A potential effects on solute ordering in a series of binary 6OCB–8OCB mixtures

E. Elliott Burnell, Ronald Y. Dong, Adrian C.J. Weber, Xuan Yang, and Anand Yethiraj

**Abstract:**  $^1\text{H}$  NMR and optical microscopy have been used to study four solutes dissolved in samples of a binary mixture of 4-*n*-hexyloxy-4'-cyanobiphenyl (6OCB) and 4-*n*-octyloxy-4'-cyanobiphenyl (8OCB) that are close to the region of the phase diagram where the smectic-A (SmA) and re-entrant nematic (RN) phases exist. Optical microscopy clearly indicates that one of the four studied samples shows the phase sequence of isotropic–nematic–SmA–RN. The derived solute order parameters were interpreted by means of two Maier–Saupe mechanisms in conjunction with the Kobayashi–McMillan theory in the case of the SmA phase. The novel feature of this study is that the nematic potential is extrapolated from the nematic to the SmA phase based on concentrations of the 6OCB–8OCB mixtures. The derived smectic order parameters for each of the studied solutes clearly show a maximum absolute magnitude near the centre of the SmA temperature range. The different partitioning of these solutes in the binary mixture is also discussed.

**Key words:** re-entrant nematic, smectic, nematic, NMR, optical microscopy, phase transition, order parameter.

**Résumé :** On a fait appel à la RMN du  $^1\text{H}$  et à la microscopie optique pour étudier quatre solutés dissous dans des échantillons d'un mélange binaire de 4-hexyloxy-4'-*o*-cyanobiphényle (6OCB) et de 4-octyloxy-4'-*o*-cyanobiphényle (8OCB) qui sont près de la région du diagramme de phase dans laquelle les phases smectique-A (SmA) et nématique réentrante (NR) existent. La microscopie optique indique clairement qu'un des quatre échantillons étudiés présente une séquence de phase d'isotrope, nématique, smectique A et nématique réentrante. On a interprété les d'ordre de solutés qui en ont été dérivés à l'aide de deux mécanismes de Maier–Saupe en relation avec la théorie de Kobayashi–McMillan dans le cas de la phase smectique A. La caractéristique nouvelle de cette étude réside dans le fait que le potentiel nématique est extrapolé de la phase nématique à la phase SmA en se basant sur les concentrations des mélanges 6OCB–8OCB. Les paramètres d'ordre smectique dérivés pour chacun des solutés étudiés montre clairement la présence d'une amplitude absolue maximale près du centre de la plage de température smectique A. On discute aussi des diverses répartitions de ces solutions dans le mélange binaire.

**Mots-clés :** nématique réentrante, smectique, nématique, RMN, microscopie optique, transition de phase, paramètre d'ordre.

[Traduit par la Rédaction]

## Introduction

Molecular orientational ordering in the nematic (N) phase, and in addition positional ordering in the case of smectic phases, is important to the basic understanding of liquid crystals (LCs).<sup>1–4</sup> Mean-field theories have been quite successfully applied for the qualitative understanding of this molecular ordering. However, careful quantitative studies of solutes in the N phase have indicated the existence of multiple ordering mechanisms (see ref. 5 and refs. therein). We have extended the study of molecular ordering to the smectic phase where nematic ordering remains but a new smectic or-

der parameter is born.<sup>6–10</sup> Here we have uncovered unusual behaviour — while linear extrapolation of the nematic ordering potential into the smectic phase works well for some solutes, it does not for others. In this paper we study a LC system with a N – smectic A – (re-entrant) N phase sequence<sup>8</sup> where the smectic range is variable, allowing us to investigate this unusual behaviour quantitatively.

To investigate the mechanisms responsible for the anisotropic ordering of molecules in condensed mesophases, it is necessary to write down the relevant intermolecular potential(s). Though there are numerous different types of shape anisotropy in the

Received 18 November 2010. Accepted 21 January 2011. Published at www.nrcresearchpress.com/cjc on 4 August 2011.

**E.E. Burnell, A.C. Weber, and X. Yang.** Department of Chemistry, University of British Columbia, 2036 Main Mall, Vancouver, BC V6T 1Z1, Canada.

**R.Y. Dong.** Department of Physics and Astronomy, University of British Columbia, 6224 Agricultural Road, Vancouver, BC V6T 1Z1, Canada.

**A. Yethiraj.** Department of Physics and Physical Oceanography, Memorial University, St. John's, NL A1B 3X7, Canada.

**Corresponding author:** E.E. Burnell (e-mail: elliott.burnell@ubc.ca).

*This article is part of a Special Issue dedicated to Professor Roderick E. Wasylshen.*

constituent molecules forming LCs, only the simplest kind, the rodlike mesogen, will be considered here. Even so, the molecules are usually composed of a rigid aromatic core, flanked by one or two flexible hydrocarbon chains. To a first approximation, it suffices to treat them as axially symmetric rods as is done in the Maier–Saupe (MS) nematic mean-field potential,<sup>11,12</sup> in which the dispersive energy is written in terms of a second Legendre polynomial  $P_2(\cos\theta_L)$  with  $\theta_L$  being the angle between the rod long axis and the nematic director  $\mathbf{n}$ . In the smectic-A (SmA) phase, there is translational ordering as molecules tend to form layers. The director is along the layer normal. To extend the MS mean-field potential to the SmA phase, Kobayashi–McMillan (KM) theory<sup>13–15</sup> adds additional terms to account for a one-dimensional density wave in the direction of the layer normal, and for a coupling between the layering and the orientational potential. The MS–KM SmA potential contains, therefore, the two interaction prefactors  $\tau'_L$  and  $\kappa'_L$  for the positional ordering and for its coupling to the orientational ordering, respectively. It is only in recent years that attempts have been made to determine these prefactors, as reported in the literature.<sup>6–10,16,17</sup>

Liquid crystals exhibiting smectic phases are invariably composed of large and flexible molecules that impose complexity in their ability to probe the intermolecular potential. One very successful approach to studying the anisotropic potential is to use small solute molecules as probes of the anisotropic environment. The size and shape of rigid solutes can be chosen to optimize their sensitivity to the orientational and (or) positional order. This has been most successful in conjunction with nuclear magnetic resonance (NMR) spectroscopy studies of the solutes.<sup>3,18</sup> In particular, in 2004 it was reported that the temperature dependence of the asymmetry in the orientational order parameters of solutes showed a distinct change on passing from the N to the SmA phase of a cyanobiphenyl.<sup>6</sup> The MS–KM theoretical approach was used to rationalize the dipolar couplings (or order parameters) of several solutes.

The experimental dipolar couplings of a solute can be used to obtain the independent second-rank order parameters, and since the number of independent order parameters equals the number of unknowns in the nematic potential, it is impossible to isolate the nematic and smectic mean-field potentials simply based on the available orientational order parameters. Thus, at a given temperature in the SmA phase, the number of unknowns in the SmA interaction Hamiltonian will always be two greater than the number of experimentally determined orientational order parameters, these unknowns being the nematic terms plus the two smectic prefactors. Crucial assumptions and approximations have to be made to make the problem solvable in terms of the smectic prefactors in the solute's smectic potential. To extract information on the KM potential from NMR experiments on the SmA phase, some details of the nematic potential in this phase must be known.

The effect of the smectic phase is clearly observed as a discontinuity in the slope at the N–SmA phase transition in plots of solute order parameter asymmetry versus quantities such as temperature, order parameter, or mean-field energy parameter. In the first attempts to utilize this observation it was assumed that the temperature behaviour of the asymmetry  $b_s$  of a molecular property tensor  $\beta_s$  for each solute in the N

phase could be extrapolated to lower temperatures where the sample is in the SmA phase. In ref. 6 linear extrapolation of  $b_s$  vs  $\beta_{s,xx}$  was used for two different solutes. Later, it was noted that such a linear procedure is not general, and could not, for example, be applied to the solute *ortho*-dichlorobenzene (odcb),<sup>7</sup> because for that solute the nematic points for  $b_s$  versus  $\beta_{s,xx}$  are curved.

In an attempt to address the curvature problem, a binary mixture of 4-*n*-hexyloxy-4'-cyanobiphenyl (6OCB)–4-*n*-octyloxy-4'-cyanobiphenyl (8OCB) was chosen because of its ability to form a re-entrant nematic (RN) phase at temperatures below the SmA phase. The hope was to see if the contiguity of behaviour between the two N phases would inform us about the validity of the extrapolation. A polynomial curve that went through all nematic points, including those in the RN phase, was drawn for odcb. When a reasonable value of  $\sim 0.3$  is chosen for solute smectic–orientational order coupling  $\kappa'$ , a successful global fit to all the temperatures can be carried out with the MS–KM potential.<sup>8</sup>

All these studies involved progressively improved strategies to extract meaningful values for solute smectic order parameters  $\tau$ . To gauge the goodness of various approximations, let us consider the smectic order parameter values of *para*-dichlorobenzene (pdcB) ( $\tau_{\text{pdcB}}$ ) in the middle of the SmA phase in 8OCB and the 6OCB–8OCB mixture:  $-0.29$ ,<sup>6</sup>  $-0.25$ ,<sup>7</sup> and  $-0.35$ .<sup>8</sup> It is interesting to see that for this particular solute, the various  $\tau$ s are comparable, indicating the suitability of the KM mean-field potential at the molecular level.

However, there is a major difficulty with the studies above. If only one MS mechanism is responsible for the nematic potential, then the solute property anisotropy ( $b_s$ ) should not show any temperature dependence. Thus, the observed temperature dependence of  $b_s$  indicates that two or more ordering mechanisms are operating in the N phase. In this regard, we note a recent study of eight solutes in seven N solvents (including a “magic mixture” for which there is evidence that solute orientational order arises from a single mechanism that involves only short-range size and shape interactions) demonstrated that solute orientational order can be rationalized to an excellent extent (agreement between experimental and calculated orientational order parameters to 5% and better) with the idea of two independent MS potentials, the so-called MSMS potential. In this potential the traceless  $\beta_{ii}$  ( $i = x, y, z$ ) are solute properties that are taken to be different for the two mechanisms, but independent of temperature. The first mechanism is taken to be associated with short-range size and shape interactions (which is then the only mechanism in the magic mixture), and the second mechanism is taken to account for additional interactions in other N samples.<sup>5</sup>

The success of the MSMS approach in the N phase prompted us to extend its application over a wider nematic temperature range, and also to apply it to the SmA phase of two LCs.<sup>9,10</sup> The molecular  $\beta_{ii}$  properties for the two MS mechanisms were determined for each solute from joint fits to order parameters of these solutes in the nematic LCs *p*-ethoxybenzylidene-*p'*-*n*-butylaniline (EBBA), Merck ZLI-1132 (1132), a magic mixture of 55 wt% 1132 and 45 wt% EBBA, and at three temperatures in each of 4-*n*-octyl-4'-cyanobiphenyl (8CB) and 8OCB. These  $\beta_{ii}$  are then taken as molecular constants, and the MSMS potential was used in

conjunction with the order parameters of 11 or 12 solutes to give  $G_{L,ZZ}^{MS_1} \equiv G_1$  and  $G_{L,ZZ}^{MS_2} \equiv G_2$  as the two fitting parameters for the nematic potential at each temperature studied in the N phase. It was then assumed that a plot of  $G_1$  vs  $G_2$ , which is essentially linear in the N phase, can be extrapolated into the SmA phase, thus providing a description of the nematic potential in the SmA phase. In the SmA phase, a combined MSMS–KM theory is then applied to gain information on the solute prefactors  $\tau'_s$ ,  $\kappa'_1$ , and  $\kappa'_2$ . Note that the  $\kappa'_i$  account for coupling to the two nematic potentials and are LC properties.

This latest work tries to address two problems associated with earlier work: the need to incorporate two nematic mechanisms, and the extrapolation involving nonlinear results. However, extrapolation (of  $G_1$ ) is still employed. In addition, to obtain a successful fit to all solute orientational order parameters obtained in the SmA phase, restrictions (upper limits) had to be placed on some  $\tau'_s$  values.

For all the studies above,  $\kappa'$  (or  $\kappa'_1$ ) were chosen to be positive; the signs of the prefactors  $\kappa'$  and  $\tau'_s$  are correlated in the smectic potential (a change of sign of all prefactors yields exactly the same result). Choosing  $\kappa'$  (or  $\kappa'_1$ )  $> 0$  is consistent with mechanism 1 being taken to be associated with size and shape interactions<sup>5</sup> that might be expected to lead to greater orientational order in the centre of the smectic layer. With the MSMS–KM approach,  $\tau_{pdcb}$  in the middle of the SmA phase of 8OCB is ca.  $-0.18$ ,<sup>9,10</sup> marginally lower than the values reported in the earlier studies.

The ability to detect, directly or indirectly, the location of solutes in layered phases is of increasing importance both because of the accessibility to this kind of information in large-scale simulations, as well as its biophysical relevance. In an attempt to better define the nematic potential in the SmA phase without the limitation imposed by extrapolation of the temperature dependence of nematic properties into the SmA phase, we again rely on the use of binary mixtures of 6OCB and 8OCB.<sup>8</sup> To this end, we have examined the NMR spectra of five solutes (1,3,5-trichlorobenzene (tcb), pdcb, odcb, *para*-bromobenzonitrile (pbbn), and phenylacetylene (phac)) dissolved in the same NMR tube for four different binary mixtures that are all close to the region in the phase diagram where a RN phase is observed; only one of the samples exhibits a stable SmA phase in microscopy studies. Although we still need to extrapolate nematic properties, it is now done as a function of small changes in LC composition, and no longer as a function of temperature.

## Theory

For the solvent, the MS potential is given by:

$$[1] \quad H_{N,L}(\theta_L) = -v_L S_L \left[ \frac{3}{2} \cos^2(\theta_L) - \frac{1}{2} \right]$$

where  $S_L$  is the solvent order parameter, and  $v_L$  governs the strength of the intermolecular interaction. The corresponding potential for a solute  $s$  (of symmetry sufficient that it has a maximum of two independent second-rank orientational order parameters) in an axially symmetric LC mean field can be written as

$$[2] \quad H_{N,Ls}(\Omega_s) = -\frac{3}{4} G_{L,ZZ} \sum_{\gamma} \sum_{\delta} \cos(\theta_{s,\gamma}) \cos(\theta_{s,\delta}) \beta_{s,\gamma\delta} \\ = -\frac{3}{4} G_{L,ZZ} \beta_{s,zz} \left\{ \left[ \frac{3}{2} \cos^2(\theta_s) - \frac{1}{2} \right] + \frac{b_s}{2} \sin^2(\theta_s) \cos(2\phi_s) \right\}$$

where  $\theta_{s,\gamma}$  is the angle between the molecular  $\gamma$  axis with respect to the nematic mean-field direction,  $G_{L,ZZ}$  is proportional to  $S_L$  with  $Z$  being the mean-field symmetry axis, and  $\theta_s$  and  $\phi_s$  are the polar and azimuthal angles of the mean-field direction in the solute ( $xyz$ ) axis system. Thus,  $G_{L,ZZ}$  is the mean-field potential of the solvent, taken to be a purely LC property, and the tensor  $\beta_s$  is taken to be a purely molecular property. The asymmetry in this solute energy parameter  $\beta_{s,ii}$  is given by

$$[3] \quad b_s = \frac{\beta_{s,xx} - \beta_{s,yy}}{\beta_{s,zz}}$$

There are thus two unknown parameters ( $G_{L,ZZ}$ ,  $\beta_{s,zz}$ , and  $b_s$ ) needed to define the nematic potential. Solutes of lower symmetry may have up to five independent second-rank order parameters (or two principal order parameters plus three diagonalization angles): the number of unknowns in the potential equals the number of independent order parameters. Up to now only solutes with at most two unknown order parameters have been used in investigations of SmA phases.

The nematic order parameter  $S_L$  for the N solvent  $L$  can be evaluated using the MS potential  $H_{N,L}(\theta_L)$  of eq. [1]:

$$[4] \quad S_L = \frac{\int \sin(\theta_L) d\theta_L \left[ \frac{3}{2} \cos^2(\theta_L) - \frac{1}{2} \right] e^{-H_{N,L}(\theta_L)/k_B T}}{\int \sin(\theta_L) d\theta_L e^{-H_{N,L}(\theta_L)/k_B T}}$$

Given the corresponding MS potential  $H_{N,Ls}(\Omega_s)$  of eq. [2] for a solute in a LC, the  $\gamma\delta$  components of the solute order parameters are given by

$$[5] \quad S_{s,\gamma\delta} = \frac{\int d\Omega_s \left[ \frac{3}{2} \cos(\theta_{s,\gamma}) \cos(\theta_{s,\delta}) - \frac{1}{2} \right] e^{-H_{N,Ls}(\Omega_s)/k_B T}}{\int d\Omega_s e^{-H_{N,Ls}(\Omega_s)/k_B T}}$$

If we now assume that the nematic potential consists of two independent MS terms, the MSMS case, then the nematic potential for solute  $s$  and LC  $L$  is

$$[6] \quad H_{N,Ls}(\Omega_s) = -\frac{3}{4} \sum_{i=1}^2 G_{L,ZZ}(i) \beta_{s,zz}(i) \\ \times \left\{ \left[ \frac{3}{2} \cos^2(\theta_s) - \frac{1}{2} \right] + \frac{b_s(i)}{2} \sin^2(\theta_s) \cos(2\phi_s) \right\}$$

$$[7] \quad H_{N,Ls}(\Omega_s) = H_{MS_1} + H_{MS_2}$$

where  $G_{L,ZZ}(1) \equiv G_1$  and  $G_{L,ZZ}(2) \equiv G_2$  as used in the Introduction and  $b_s(i)$  is still the solute energy asymmetry expressed according to eq. [3] with index  $i$  to distinguish the two different LC/solute interactions.  $G_{L,ZZ}(i) \beta_{s,zz}(i)$  could be the short-range size and shape effects or longer range

interactions such as that involving the LC average electric field gradient interacting with the solute quadrupole or the solute polarizability with the mean square electric field. We will use, in this study, the Hamiltonian of eq. [6] to evaluate solute order parameters  $S_{s,\gamma\gamma}$  in the N phase based on eq. [5].

Following the success of the MSMS–KM theory in treating solutes in the SmA phases of 8CB and 8OCB, the smectic interaction potential is written as before,<sup>9,10</sup>

$$[8] \quad H_{A,Ls}(\Omega_s, Z) = H_{MS_1} \left[ 1 + \kappa'_1 \cos\left(\frac{2\pi Z}{d}\right) \right] + H_{MS_2} \left[ 1 + \kappa'_2 \cos\left(\frac{2\pi Z}{d}\right) \right] - \tau'_s \cos\left(\frac{2\pi Z}{d}\right) \\ = H_N^{\text{mod}}(1) + H_N^{\text{mod}}(2) - \tau'_s \cos\left(\frac{2\pi Z}{d}\right)$$

where the prefactors  $\kappa'_1$  and  $\kappa'_2$  denote coupling between the nematic potential and the density wave for the two MS mechanisms (each  $\kappa'$  can in principle be temperature dependent), whereas the solute smectic prefactor  $\tau'_s \equiv \tau'$  is the coupling strength for a solute to feel the smectic layering of the solvent molecules. The layer width is  $d$  and  $Z$  ( $Z = 0$  in the centre of a layer) is along the layer normal. The observed orientational order parameters can be calculated based on this potential by the following expression,

$$[9] \quad S_{s,\gamma\gamma} = \frac{\int d\Omega_s \int_0^d \left[ \frac{3}{2} \cos^2(\theta_{s,\gamma}) - \frac{1}{2} \right] e^{-H_{A,Ls}(\Omega_s, Z)/k_B T} dZ}{\int d\Omega_s \int_0^d e^{-H_{A,Ls}(\Omega_s, Z)/k_B T} dZ}$$

This would allow us to determine the prefactors in the smectic potential provided that one has prior knowledge of  $H_{MS_1}$  and  $H_{MS_2}$  at the temperature of interest in the SmA phase. Fortunately the  $\beta_{s,\gamma\gamma}(1)$  and  $\beta_{s,\gamma\gamma}(2)$  for the solutes studied have been carefully determined from studies of these solutes in several LCs including 8OCB<sup>10</sup> and can be taken as constants for the current binary mixtures of 8OCB–6OCB. However, the  $\beta$  values alone are not sufficient to give the nematic potential: one also must know the values of  $G_1$  and  $G_2$  at the desired temperature in the SmA phase. In this earlier study it was assumed that a plot of  $G_1$  vs  $G_2$  could be extrapolated from the N (where it is linear) into the SmA phase. In the present case,  $G_1$  and  $G_2$  have been obtained experimentally (vide infra).

Once the full smectic potential  $H_{A,Ls}(\Omega_s, Z)$  is known,  $\tau$  can be easily evaluated according to

$$[10] \quad \tau_s \equiv \tau = \frac{\int d\Omega_s \int_0^d \cos\left(\frac{2\pi Z}{d}\right) e^{-H_{A,Ls}(\Omega_s, Z)/k_B T} dZ}{\int d\Omega_s \int_0^d e^{-H_{A,Ls}(\Omega_s, Z)/k_B T} dZ}$$

The mixed order parameters (for  $\kappa$  coupling) can in principle be calculated for each solute, but there are many of them and they seem not to give any additional insight like the translational order parameter  $\tau$ .

## Experimental

The solutes odcb, phac, pdcb, pbbn, and tcb were dissolved into LCs 8OCB and 6OCB. Enough of each solute was mixed thoroughly in the isotropic phase to obtain 1 mol%

per solute and a total of 4 g of each LC was prepared in this way. Both LCs were degassed and then kept in the N phase with the use of a warm water bath. To span the two-component 8OCB–6OCB phase diagram a series of samples were made with varying relative weight fraction ( $w_{6OCB}$ ) of the two LCs. In this way the solute concentrations were as equal as possible in all samples studied. Enough of each sample was made so that <sup>1</sup>H NMR and microscopy could be performed on the same sample. For NMR studies, each sample was thoroughly mixed, and part placed into a 5 mm o.d. NMR tube and the rest into a glass ampule, both being sealed under nitrogen. Ten samples were made of differing  $w_{6OCB}$ . The compositions of those investigated were  $w_{6OCB} = 0.270$  (sample 4), 0.297 (sample 6), 0.301 (sample 7), and 0.318 (sample 8). The phase-transition sequence in each sample was independently monitored via cross-polarizer optical microscopy.

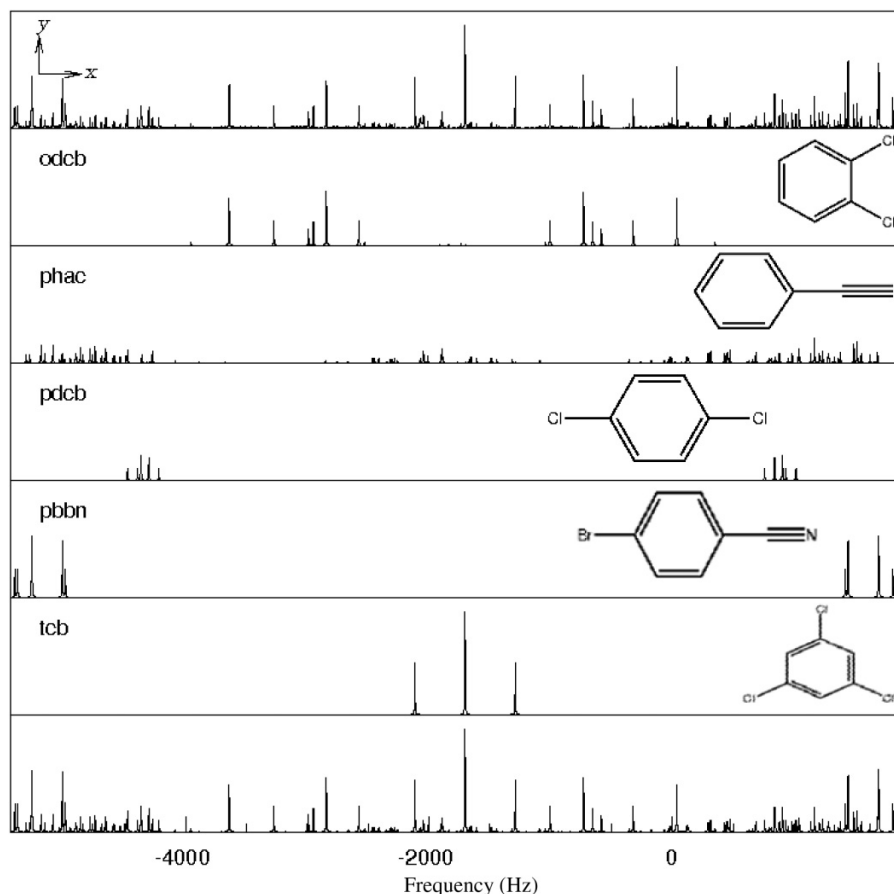
For microscopy studies, samples were prepared between No. 1 cover slips, using strips of No. 0 cover slips (~100  $\mu\text{m}$ ) as spacers. Samples were sealed using Norland epoxy NOA 68 and cured under a UV lamp. Samples for microscopy experiments were heated to the N phase and placed atop an aluminium baseplate with a circular window and inside an Instek HCS 61 hot stage, which was mounted on a Nikon Eclipse 80-i upright microscope equipped with crossable polarizing filters. White light transmission cross-polarizer micrographs were obtained using a Qimaging QICAM Fast 1394 12-bit monochrome camera. The hot-stage temperature was changed in a controlled slow ramp (2  $^\circ\text{C}/\text{min}$ ), and images were acquired and saved to disk at 10 s intervals.

Samples for NMR experiments were heated to the N phase, mixed and then placed into a Bruker Avance 400 MHz NMR spectrometer magnet in which the director was oriented by the magnetic field along the field direction. With the temperature controlled by the Bruker air-flow system, spectra were acquired in 0.5 and 1 K steps throughout both N and SmA phases. The spectral parameters (dipolar couplings ( $D_{ij}$ ) and chemical shifts ( $\omega_i$ )) of the solutes were then obtained simultaneously and automatically with the use of a covariance matrix adaptation evolution strategy (CMA-ES)<sup>9,19–21</sup> for each LC mixture at each temperature. Figure 1 shows the NMR spectra of solutes in sample 4 at 339.5 K. The upper plot shows the experimental proton NMR spectrum, whereas the lower plot is a sum of the calculated spectra of the studied solutes. As seen from these, the calculated spectrum agrees very well with the experimental spectrum obtained at 400 MHz. The dipolar couplings obtained from the analysis, in conjunction with the solute geometries,<sup>22–25</sup> were then used to determine the solute order parameters, which are given in the Supplementary data. No corrections were made for molecular vibrations and other nonrigid effects.

## Results and discussion

First, the phase sequence of the samples was verified by optical microscopy. Characterization of the phase-transition sequence by optical microscopy utilizes the dramatic differences in defect textures in the N and smectic phases. Sample 4 was the only one to exhibit an unambiguous I–N–SmA–RN phase sequence. Figure 2 shows cross-polarizer optical micrographs of sample 4 at different temperatures corresponding to N,

**Fig. 1.**  $^1\text{H}$  NMR spectra of solutes in sample 4 at 339.5 K. The upper plot is of the experimental 400 MHz NMR spectrum and the bottom plot is a sum of the calculated spectra. The calculated spectra of the solutes from top to bottom are *ortho*-dichlorobenzene (odcb), phenylacetylene (phac), *para*-dichlorobenzene (pdcb), *para*-bromobenzonitrile (pbbn), and 1,3,5-trichlorobenzene (tcb), with the molecule-fixed coordinate system being found in the top left of the figure.



SmA, and RN phases. Note that there is no detectable difference between the N and the RN phases, but the defect textures in the SmA phase are very distinct. Sample 6 was not observed to form a stable smectic phase, but exhibited clear signs of smectic fluctuations over a 3 °C temperature range. It is quite feasible that these fluctuations are present because of proximity to the critical point in the phase diagram beyond which the SmA phase no longer exists. Sample 8 showed no evidence of a smectic phase.

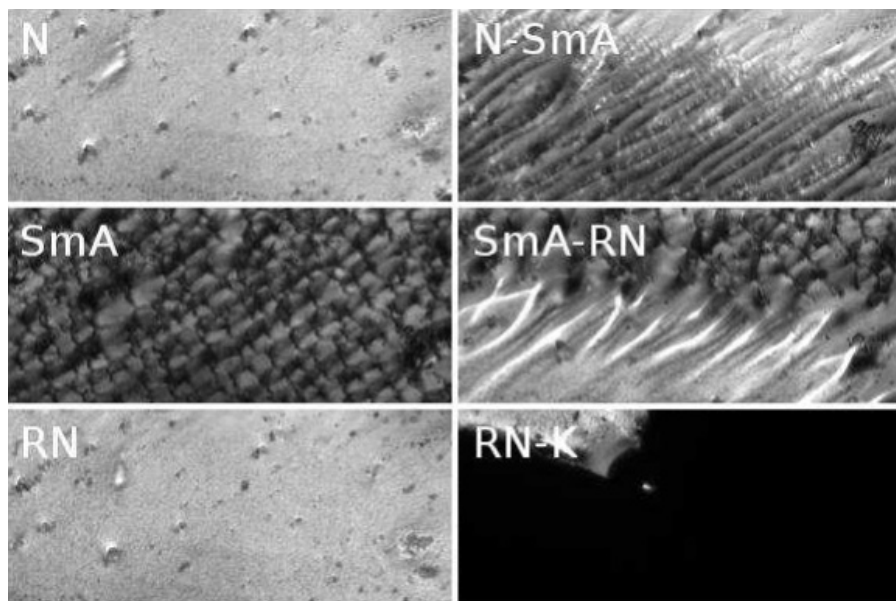
The set of solute order parameters obtained for each NMR experiment in both the N and SmA phases were fitted in a minimization to the MSMS nematic potential of eq. [6] to obtain  $G_1$  and  $G_2$  values (results not shown). In these fits the solute  $\beta$  parameters are taken from ref. 10. For samples that are clearly in the N phase, the two largest in absolute value order parameters for each solute recalculated from the  $G$  fit parameters agree with the experimental ones to better than 5%, except for  $S_{yy}$  (odcb) where the deviation is ~8% at lower temperatures. This excellent agreement confirms once again the validity of the MSMS potential<sup>5</sup> for the N phase, and that the solute  $\beta$  parameters are valid in the 6OCB–8OCB mixtures. However, the effect of the SmA phase on the orientational order parameters is quite small, and here we need to account for the nematic potential in as accurate a manner as

possible; the 5% agreement achieved by the MSMS potential is not nearly sufficient for this purpose.

Deviations from the MSMS potential arise from a possible temperature dependence of the solute  $\beta_{ii}$  parameters and (or) deficiencies of the model in terms of different solutes experiencing different LC mean fields  $G$  as the temperature varies. We keep the main result of the MSMS potential, that two different MS mechanisms are sufficient to characterize the nematic potential; we arbitrarily choose to use the  $\beta_{ii}$  values determined earlier<sup>10</sup> and to obtain an exact fit to the order parameters by adjusting the  $G$  values separately for each solute in each sample at each temperature. This is an arbitrary choice, but as only the products  $G\beta$  contribute to the potential (meaning that it is impossible to separate unambiguously  $G$  from  $\beta$ ), making  $G$  values a function of both solute and solvent to get an exact fit to all solute order parameters in the N phase is as valid a choice as any. Hence, we do not need to worry about the precise nature of the  $G\beta$  products involved with the MSMS potential.

Earlier studies attempted to characterize the nematic potential in the SmA phase by extrapolation of  $G$  parameters from the N into the SmA phase.<sup>9,10</sup> Here we use a different approach — we explore the possibility of estimating the nematic potential in the SmA phase by extrapolation as a

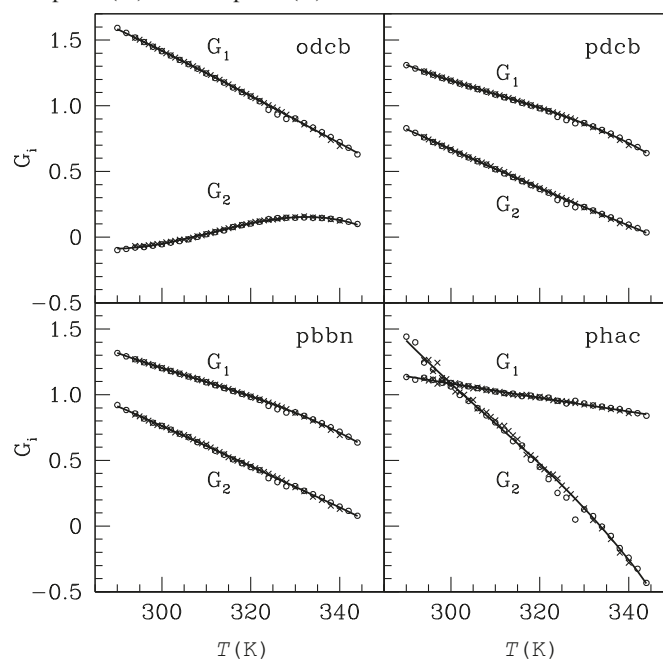
**Fig. 2.** Characterization of phase transition by optical microscopy utilizes the dramatic differences in defect textures in the nematic (N) and smectic (SmA) phases. Snapshots (at temperatures  $T = 317.6, 316.7, 311.8, 296.9, 292.0,$  and  $283.7$  K, respectively) from the complete time series (included as a movie in Supplementary data) show the N phase, N–SmA interface, SmA phase, SmA–RN interface, RN phase, and the RN–crystal (RN–K) interface.



function of LC composition (a different extrapolation for each temperature). We use the two order parameters for each solute  $s$  (except tcb, which has a single order parameter and therefore is not used because one order parameter cannot be used to determine two  $G$  values) and the MSMS nematic potential (eq. [6]) with the  $\beta_{ii}$  parameters determined earlier<sup>10</sup> to find values for the nematic potential parameters  $G_1$  and  $G_2$  for each solute in each experiment (including those for samples that show the SmA phase). The results for samples 7 ( $w_{60CB} = 0.301$ ) and 8 ( $w_{60CB} = 0.318$ ) (which from microscopy are clearly in the N phase at all temperatures investigated) are presented in Fig. 3. Even though  $w_{60CB}$  is different for these two samples, the  $G$  parameters are to an excellent degree equal. This is taken as affirmation that the nematic  $G$  parameters can be taken to be constant over the small concentration range ( $w_{60CB} = 0.270$  for sample 4 to  $w_{60CB} = 0.318$  for sample 8) spanned by the samples studied here. In other words, as samples 7 and 8 (which do not exhibit a SmA phase) give essentially equal  $G$  values for a given temperature, we assume that these values can be used as the nematic  $G$  values for the same temperatures in samples 4 and 6. To facilitate this idea, we do a polynomial fit to the  $G$  vs  $T$  values for samples 7 and 8. The lines drawn through the points in Fig. 3 are these polynomial fits.

Figure 4 presents the fitting parameters  $G_1$  and  $G_2$  vs  $T$  obtained by fitting the nematic potential only to order parameters obtained for solutes in samples 4 and 6, as well as the polynomial fit lines obtained from samples 7 and 8. The smectic effects are clearly seen at lower temperatures in samples 4 and 6, particularly between 296.9 and 316.7 K in sample 4 (the temperature range in which the SmA phase is observed with microscopy) where the points deviate dramatically from the lines. The most notable effects are noticed for the odcb and phac  $G_2$  values in sample 4, but are observable elsewhere with close inspection. The broken lines in this (and

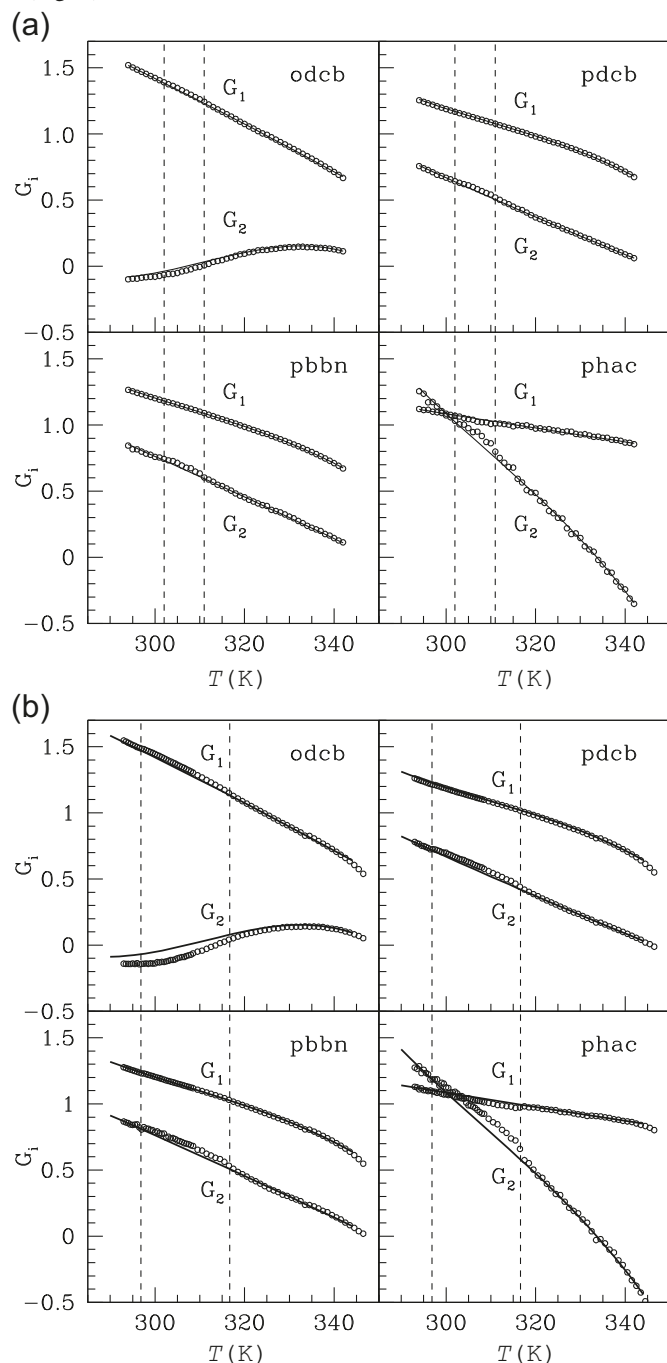
**Fig. 3.**  $G_1$  and  $G_2$  derived with the nematic potential (eq. [6]) only in samples 7 and 8. Lines denote polynomial fits to the  $G$  values. Sample 7 (O) and sample 8 (X).



other) graphs denote either the temperature range in which the SmA phase was observed with microscopy (sample 4) or a range close to the SmA phase region (sample 6). At higher temperatures the polynomials go through the points, justifying the transfer of nematic potential parameters among samples.

Hence, we take deviations from the lines as being caused by the smectic part of the interaction Hamiltonian. Smaller deviations are observed for sample 6 for which no smectic

**Fig. 4.** The points are  $G_1$  and  $G_2$  from fits of the nematic potential only (eq. [6]) to orientational order parameters for sample 6 (a) and sample 4 (b) vs  $T$ . The solid lines are polynomial fits to  $G_1$  and  $G_2$  values determined for fits of the nematic potential to samples 7 and 8 (Fig. 3).



phase is observed in the microscopy experiments; however, “critical” fluctuations are observed in the region in the phase diagram that is near the smectic phase.

Thus, to fit the solute order parameters for each experiment of samples 4 and 6 to the SmA potential, the nematic  $G_1$  and  $G_2$  parameters in the total potential for the SmA phase (eq. [8]) are taken from the polynomial fit lines to the pure N samples 7 and 8, and the values of the smectic

parameters  $\kappa'_1$ ,  $\kappa'_2$ ,  $\tau'_{\text{odcb}}$ ,  $\tau'_{\text{pdc}}$ ,  $\tau'_{\text{pbb}}$ , and  $\tau'_{\text{phac}}$  are optimized for best fits at each temperature. The  $\kappa'_i$  values obtained are given in Fig. 5 and the  $\tau'$  values are reported in the Supplementary data. As discussed earlier,  $\kappa'_1$  is taken to be positive, consistent with higher shape-dependent ordering in the middle of a smectic layer. As expected, larger effects are noticed for sample 4. The phase transitions can also be noticed in Fig. 5. Values obtained from fits in the N phase should be zero: while the fitted numbers are not zero, they are associated with rather large errors, indicating the absence of the SmA phase.

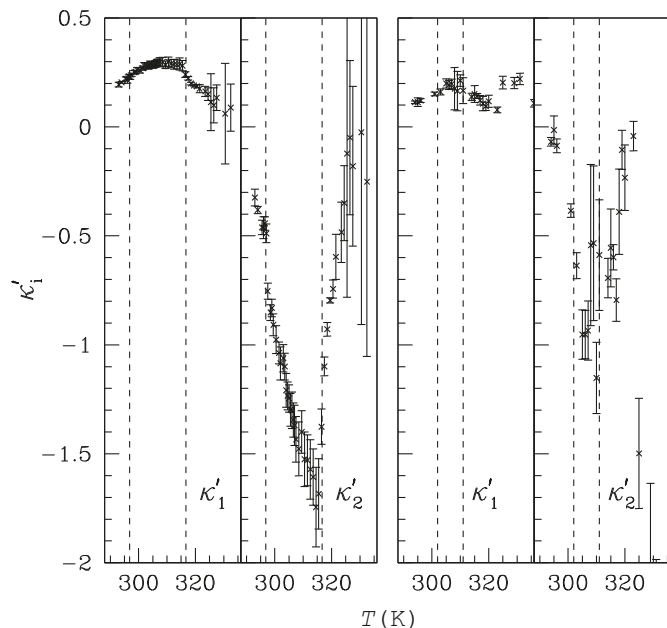
The  $\tau$  obtained for each solute in each experiment are given in Fig. 6. The sign of these parameters generally agrees with those determined from the earlier studies that relied on extrapolation of nematic parameters from the higher temperature N phase. It is encouraging that the essence of the analysis of the effects of a smectic phase on orientational order parameters was correct, even with the inherent dangers involved with the necessity of an extrapolation with temperature. Here we also do an extrapolation, i.e., we assume that the nematic  $G\beta$  parameters are constant with sample composition.

The earlier study<sup>10</sup> that used the MSMS–KM theory with solutes dissolved in 8CB and 8OCB ran into difficulties with determination of  $\tau$ , and in some cases limiting values had to be placed on some  $\tau'$  values. The present approach does not require such restrictions. Here each SmA experiment is analysed by itself (given the nematic parameters). It is assumed that all solutes have the same  $\kappa'$  values, i.e., that  $\kappa'$  is a LC property, and that each solute has its own smectic prefactor  $\tau'$ .

As is seen in Fig. 5,  $\kappa'_1$  and  $\kappa'_2$  have opposite sign, this being the same result observed in the earlier study that used the MSMS–KM approach.<sup>10</sup> The general trends in the results for sample 6 are quite similar to those for sample 4, but  $\kappa'$  absolute values are smaller and errors are larger; these observations are consistent with sample 4 exhibiting a SmA phase and sample 6 exhibiting only pretransitional effects. We note that  $\kappa'_1$  peaks in the centre of the SmA region, meaning that the variation in the nematic potential is maximum when deepest into the smectic phase, as might be expected. The values are not exactly zero in the N regions, especially in the RN region, indicating either a slight breakdown of the assumption that the nematic  $G$  parameters are identical in all samples or the existence of a correlation between  $\kappa'$  and  $\tau'$  in the KM smectic potential. We recall that the  $\beta_{ii}$  parameters used in the analysis are based on mechanism 1 being associated with short-range size and shape interactions. The relatively small ( $\approx 0.3$ ) values of  $\kappa'_1$  are consistent with this notion, as this value means a change of roughly a factor of 2 when a solute goes from the rather rigid region in the centre of a smectic layer (large nematic potential) to the rather disordered region between layers where the nematic potential is expected to be reduced.

The N–SmA phase transitions are clear in the plot of  $\kappa'_2$  vs  $T$ . It is interesting that  $\kappa'_2$  becomes increasingly more negative with increasing  $T$  within the SmA phase. Its absolute value exceeds 1, which means there is a change in sign of the nematic potential as solutes go through a smectic layer. This same change of sign was observed in the earlier study

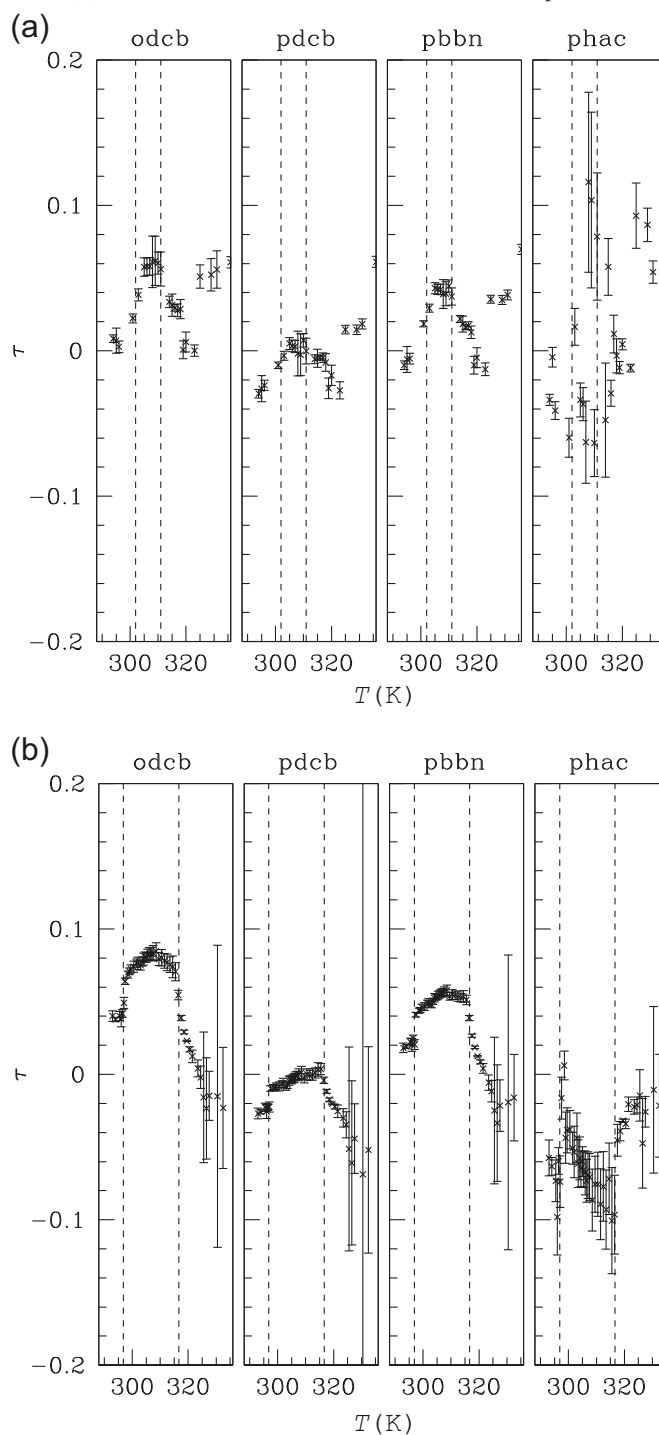
**Fig. 5.**  $\kappa'_1$ ,  $\kappa'_2$  (including errors) vs  $T$  for sample 4 (left panel) and for sample 6 (right panel). Vertical lines indicate phase transitions as measured by microscopy. The smectic-A (SmA) phase is clearly indicated by the regions of nonzero  $\kappa'$  values with smaller errors.



of solutes in 8CB and 8OCB,<sup>10</sup> where it was rationalized in terms of the angle dependence of the long-range part of the solute–solvent intermolecular interaction as a solute passes along the long axis of a solvent molecule. Possibilities for the anisotropic interactions include those involving solute and solvent quadrupoles, polarizabilities, etc. This second mechanism shows a much stronger temperature dependence than does the first (size and shape) mechanism. However, the absolute values of both  $G_2$  and  $\beta(2)$  are in general smaller than those for mechanism 1, and thus the first mechanism dominates the ordering potential. Thus, the large temperature dependence of  $\kappa'_2$  may well be associated with possible changes in the molecular packing. It could be interesting to explore simulations of solutes in the SmA phase (where, for example, interactions between solute and solvent quadrupoles are included<sup>26</sup>) to shed light on this interesting result and its temperature dependence.

The  $\tau$  order parameters give information on the partitioning of a solute within the smectic layer. With our chosen sign convention (that short-range interactions lead to a stronger nematic potential within the smectic layer), a positive  $\tau$  implies a preference for the solute to partition within the layer, and a negative sign implies partitioning between layers. The calculated  $\tau$  values (Fig. 6) for both samples 4 and 6 are quite similar, but those for sample 4 have lower error and show less scatter. The values peak in the middle of the SmA phase, and their relatively sudden changes in values agree with the N–SmA phase transitions. The values for phac have more error than those for the other solutes. The  $\tau$  values, especially in sample 4, indicate that odcb and pbbn prefer to sit within the layers and phac has values very close to zero deep in the SmA phase, implying an even distribution, and tend to be negative when near the N phase, thereby suggesting its like-

**Fig. 6.**  $\tau$  order parameters (including errors) vs  $T$  for samples 6 (a) and 4 (b). See text for details on nonzero  $\tau$  in nematic phases.



likelihood to be in between layers. It should be noted that earlier studies have found pdcB to have negative  $\tau$  as mentioned above when one (two) MS mechanism(s) was invoked to describe the nematic potential.<sup>8,10</sup>

## Conclusion

NMR results were obtained for four samples of binary mixtures with compositions very close to the region in the phase diagram where a RN phase exists at low temperature.

The microscopy experiments clearly show that one sample (sample 4) on cooling goes from an isotropic to a N to a SmA to a RN phase. Microscopy on sample 6 gives fluctuations in the N phase as the temperature passes close to the region where the SmA phase exists, but sample 6 is not observed to form a stable SmA phase. Evidence for smectic fluctuations in Sample 7 was not conclusive, whereas sample 8 showed no evidence whatsoever of a smectic phase.

Because for a given temperature the  $G$  parameters that describe the nematic potential are essentially identical for each solute in all four samples when they are in the N phase, we make the reasonable ansatz that in the SmA phase regions of samples 4 and 6 the nematic potential can be taken equal to that in samples 7 and 8 at the same temperature. We then analyzed samples that are in the SmA phase to extract the smectic prefactors  $\kappa'_1$  and  $\kappa'_2$  for the LC and a  $\tau'$  for each solute in the smectic potential based on the KM theory of SmA phases. The values obtained are then used to calculate the smectic order parameter  $\tau$  for each solute. The numbers obtained agree in general with those found in earlier studies (except odcb, which was arbitrarily set to 0.8 in the earlier studies<sup>10</sup>) that involved extrapolation of nematic potential parameters as a function of temperature into the SmA phase, a procedure fraught with potential error.

In the present study we gauge an interaction Hamiltonian to be incorrect in the N phase(s) (i.e., a Hamiltonian that includes the KM potential) by getting nonzero  $\kappa'$  and  $\tau'$  values with large errors, as can be observed in Figs. 5 and 6. As a consequence, the corresponding solute smectic order parameters  $\tau$  calculated from  $\tau'$  values in the N phase should be taken with a grain of salt. In fact, the  $\tau$  parameters should strictly vanish; the same is true for all the smectic prefactors. To summarize, the present study of binary 6OCB–8OCB mixtures that combines NMR and optical microscopy has clearly put the MSMS nematic potential in conjunction with the KM smectic potential on a firm ground for the SmA phase.

## Supplementary data

Supplementary data are available with the article through the journal Web site (www.nrcresearchpress.com).

## Acknowledgement

We thank W.L. Meerts for help with the CMA-ES spectral fitting, and the Natural Sciences and Engineering Research Council of Canada (NSERC) for financial support.

## References

- (1) Chandrasekhar, S. *Liquid Crystals*; Cambridge University Press: Cambridge, UK, 1992.

- (2) Dong, R. Y. *Nuclear Magnetic Resonance of Liquid Crystals*; 1st ed.; Springer-Verlag: New York, 1994.
- (3) Burnell, E. E.; de Lange, C. A., Eds. *NMR of Ordered Liquids*; Kluwer Academic: Dordrecht, The Netherlands, 2003.
- (4) Dong, R. Y., Ed. *Nuclear Magnetic Resonance Spectroscopy of Liquid Crystals*; World Scientific: Singapore, 2009.
- (5) Burnell, E. E.; ter Beek, L. C.; Sun, Z. *J. Chem. Phys.* **2008** *128* (16), 164901. Note that the  $S_{xx}$  values for fluorobenzene in 1132 and MM reported in Table I should both be positive. doi:10.1063/1.2900559.
- (6) Yethiraj, A.; Sun, Z.; Dong, R. Y.; Burnell, E. E. *Chem. Phys. Lett.* **2004** *398* (4–6), 517. doi:10.1016/j.cplett.2004.09.108.
- (7) Yethiraj, A.; Weber, A. C. J.; Dong, R. Y.; Burnell, E. E. *J. Phys. Chem. B* **2007** *111* (7), 1632. doi:10.1021/jp0670438.
- (8) Yethiraj, A.; Burnell, E. E.; Dong, R. Y. *Chem. Phys. Lett.* **2007** *441* (4–6), 245. doi:10.1016/j.cplett.2007.05.043.
- (9) Weber, A. C. J.; Yang, X.; Dong, R. Y.; Meerts, W. L.; Burnell, E. E. *Chem. Phys. Lett.* **2009** *476* (1–3), 116. doi:10.1016/j.cplett.2009.06.002.
- (10) Weber, A. C. J.; Yang, X.; Dong, R. Y.; Burnell, E. E. *J. Chem. Phys.* **2010** *132* (3), 034503. doi:10.1063/1.3291486.
- (11) Maier, W.; Saupe, A. *Z. Naturforsch. A.* **1959** *14*, 882.
- (12) Maier, W.; Saupe, A. *Z. Naturforsch. A.* **1960** *15*, 287.
- (13) Kobayashi, K. K. *Mol. Cryst. Liq. Cryst. (Phila. Pa.)* **1971** *13* (2), 137. doi:10.1080/15421407108084959.
- (14) McMillan, W. L. *Phys. Rev. A* **1971** *4* (3), 1238. doi:10.1103/PhysRevA.4.1238.
- (15) McMillan, W. L. *Phys. Rev. A* **1972** *6* (3), 936. doi:10.1103/PhysRevA.6.936.
- (16) Cifelli, M.; Cinacchi, G.; De Gaetani, L. *J. Chem. Phys.* **2006** *125* (16), 164912. doi:10.1063/1.2359428.
- (17) Celebre, G.; Cinacchi, G.; De Luca, G. *J. Chem. Phys.* **2008** *129* (9), 094509. doi:10.1063/1.2970074.
- (18) Burnell, E. E.; de Lange, C. A. *Chem. Rev.* **1998** *98* (6), 2359 and references therein. doi:10.1021/cr941159v.
- (19) Meerts, W. L.; Schmitt, M.; Groenenboom, G. *Can. J. Chem.* **2004** *82* (6), 804. doi:10.1139/v04-037.
- (20) Meerts, W. L.; Schmitt, M. *Int. Rev. Phys. Chem.* **2006** *25* (3), 353. doi:10.1080/01442350600785490.
- (21) Burnell, E. E.; de Lange, C. A.; Meerts, W. L. *Nuclear Magnetic Resonance Spectroscopy of Liquid Crystals*; Dong, R. Y., Ed.; World Scientific Publishing Co.: Singapore, 2009.
- (22) Syvitski, R. T.; Burnell, E. E. *J. Magn. Reson.* **2000** *144* (1), 58. doi:10.1006/jmre.1999.2013.
- (23) Dereppe, J. M.; Arte, E.; Van Meerssche, M. *J. Cryst. Mol. Struct.* **1974** *4* (4), 193. doi:10.1007/BF01198176.
- (24) Syvitski, R. T.; Burnell, E. E. *Can. J. Chem.* **1999** *77* (11), 1761. doi:10.1139/cjc-77-11-1761.
- (25) Britton, D.; Gleason, W. B. *Acta Crystallogr.* **1977** *B33*, 3926. This paper is for the structure of *p*-fluorobenzonitrile, which was used here for the proton coordinates of pbbn.
- (26) Sokolovskii, R. O.; Burnell, E. E. *J. Chem. Phys.* **2009** *130* (15), 154507 and references therein. doi:10.1063/1.3104607.